2025 25th International Conference on Process Control (PC)
June 3–6, 2025, Štrbské Pleso, Slovakia

Education Platform for Periodic Control

Tomáš Myslivec
Department of Cybernetics
Faculty of Applied Sciences
University of West Bohemia
Pilsen, Czechia

Miloš Schlegel
NTIS Research Center
Faculty of Applied Sciences
University of West Bohemia
Pilsen, Czechia

***Abstract*—This paper describes a new educational model suitable for developing and testing periodic and repetitive control. The model consists of a BLDC motor with a connected rotor optionally equipped with one or two permanent magnets, a stator with 10 cells, which can also be optionally equipped with permanent magnets, and a motor control unit. This construction allows the model to generate many load torque variants during one motor revolution. The essential task now is to design a feedback controller that ensures a constant motor rotation speed under the influence of a selected periodic disturbance. The paper further describes the individual steps of the speed controller design by gradually improving the standard PI controller with so-called PR (proportional-resonant) controllers using the design tool PID H_∞ Designer (www.pidlab.com).**

***Index Terms*—Education Platform, Periodic Control, Proportional Resonant Controller, PI Controller, Periodic Disturbances**

I. Introduction

Industrial processes frequently involve tasks, which are inherently vulnerable to disturbances. These disturbances can stem from various sources, such as material variations, environmental factors, machine wear, and tooling imperfections. Alternatively, a large class of systems is dedicated to executing repetitive tasks, including automated production lines and robotic systems. As the demand for high-quality, high-productivity systems increases, the need for precise control of these systems becomes increasingly critical. This includes a wide range of tasks, including controlling robotic manipulators, servo systems [2], stabilizing satellites, compensating for active damping [8], reading data from hard disk drives, PWM drivers and inverters for photovoltaic power plants [1], [10].

A Proportional Resonant (PR) Controller is a widely utilized control strategy in power electronics and electrical engineering, particularly for applications involving alternating current (AC) signals [3]. It also finds applications in robotics and other domains. PR controllers effectively manage sinusoidal disturbances by eliminating steady-state errors due to high gain at the prescribed frequency [13]. This enhances system performance in applications such as inverters [12], grid-connected devices [11], and active filters [14].

The Education Platform for Periodic Control presented here, is designed to facilitate the testing of control algorithms for systems subjected to periodic disturbances. This platform offers flexibility by allowing a wide range of disturbance signals through straightforward hardware modifications. Additionally, the platform prioritizes safety by incorporating a secured motor and lever enclosed within a protective ring. This design significantly reduces the safety risks compared to larger motor assemblies or robotic manipulators. It is highly advantageous for testing control algorithms for periodic control, particularly in the context of education.

II. Platform design

The primary objective was to design an affordable motion periodic platform that met several fundamental objectives:

- Reasonable purchase and maintenance costs
- Simple modular structure with easy configuration
- Safety, robustness, and easy handling
- Large range of laboratory tasks to compensate for periodic disturbances

These requirements led us to design a 3D printable stand with only key mechanical components, such as a BLDC motor, a programmable motor controller [9], and an embedded computer (Raspberry Pi 3). The stand is augmented with the software tools [7] that facilitate the design of high-quality and efficient control algorithms, thereby establishing an effective platform for periodic control.

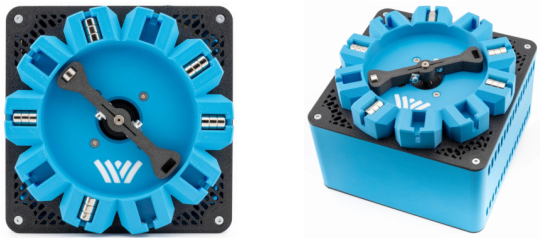

(a) Upper Ring (b) The whole model

Fig. 1: Periodic Motor Stand Model

A. Construction of the motor stand

The entire construction is divided into two distinct parts: a box containing the motor and electronic components and an upper ring with slots for neodymium permanent magnets and a motor lever (see Fig. 1). This design allows for quick replacement of the upper ring with another one and thus future modification of the model. The motor lever has two sides that can be utilized, for instance, to double the number of peaks in disturbance signal within one period.

979-8-3315-2530-9/25/$31.00 ©2025 IEEE

B. Components and software

Education platform for periodic control includes several hardware and software components to address the comprehensive requirements during the design process of advanced control systems that effectively compensate periodic disturbances.

1) Motor:

- Brushless DC motor Nanotec BD43M02430
- Rated speed 3000 rpm, rated torque 17 Ncm, rotor inertia 60 gcm^2
- Optical incremental encoder - 20 000 CPR

2) Programmable Motor Controller:

- Advanced Motion Controller v2 (AMC2)
- Powered by an embedded version of REXYGEN runtime
- Fully configurable

3) Embedded Computer:

- Raspberry Pi 3 Model B+
- 1.2 GHz quad-core processor

4) REXYGEN Control System [4]:

- Software environment for rapid real-time control prototyping based on graphical programming
- Python or C-like scripting and sequential function chart support

5) PID H_∞ Designer [5]:

- Advanced tool for the design of structured controllers with two tunable parameters (PI, PID, Lead/Lag, PR, RC)
- Analytical design based on H_∞ specifications

The hardware components are interconnected as depicted in the Fig. 2. All communication is performed by EherCAT [15], an industrial Ethernet system designed to meet stringent hard real-time requirements, ensuring deterministic response times. AMC2 is connected to a BLDC motor and utilizes an optical incremental encoder to monitor the velocity and position of the motor.

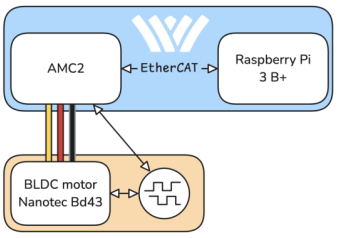

Fig. 2: Internal Connection

C. Evaluation of the platform

This project successfully developed an affordable, modular motion platform for periodic disturbance compensation in laboratory settings. By combining 3D-printed components with carefully selected hardware (BLDC motor, Raspberry Pi, and industrial-grade EtherCAT communication), it is achieved a cost-effective yet high-performance solution. The platform's interchangeable design and advanced control software (REXYGEN and PID H_∞ Designer) provide excellent flexibility for various experimental needs.

III. Stand Disturbances

As previously mentioned, the repetitive stand possesses the capability of generating a diverse range of disturbance signals by simply altering the position of the neodymium magnets. The rotor comprises two slots designed to accommodate a magnet. Each slot of the stator ring offers three distinct positions that can be occupied by a magnet or a "dummy" magnet to modify the magnetic force. Furthermore, each slot provides the possibility to use any magnet orientation. These various settings provide us with ample flexibility in selecting the appropriate disturbance signal. For the purposes of this paper, only a limited number of options will be presented. On the following figures, there are several cases of magnet distributions and velocity of motor during two revolutions (the first one is blue, and the second one is red) of the standard closed loop (PI controller).

The example (Fig. 3) involve cases combinations of multiple magnets with differently oriented poles. It demonstrates the versatility and adaptability of the stand in various configurations.

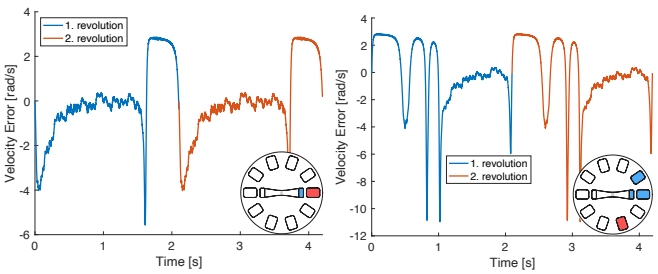

Fig. 3: Velocity signal during two motor revolutions

IV. Stand Identification

Considering the following closed loop cascade configuration (Fig. 4) of BLDC motor with two controllers, where

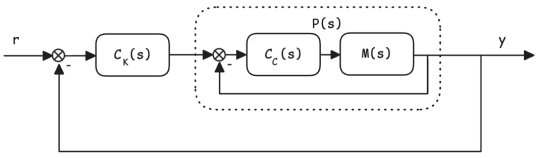

Fig. 4: Cascade configuration of the control system

$C_K(s)$ is proportional auxiliary controller for identification purpose. $P(s)$ is the transfer function corresponding to the internal current loop of the BLDC motor. The internal current loop consists of the advanced control algorithm Field Oriented Control (FOC) [19], which is widely used in BLDC motors. PI controllers inside FOC are tuned in a standard way. It is convenient to identify the transfer function P(s) based on a closed-loop experiment. For this purpose, the following closed-loop configuration is introduced.

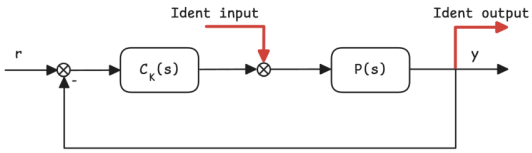

Fig. 5: Closed loop for system identification

From the input (Ident input) and output (Ident output) records (Fig. 5), using the method N4SID (Numerical Subspace State-Space System Identification, [6]) supported in the PID H_∞ Designer application, we will determine the transfer function

$$G(s) = \frac{P(s)}{1 + C_K(s)P(s)}. \tag{1}$$

From it follows, that the identified transfer function $P(s)$ is

$$P(s) = \frac{G(s)}{1 - C_K(s)G(s)}. \tag{2}$$

For BLDC motors, the utilization of a second-order transfer function $P(s)$ is recommended [18]. This approach results in

$$P(s) = k\frac{\omega_n^2}{s^2 + 2\xi\omega_n s + \omega_n^2}, \tag{3}$$

where ξ is the damping ratio, ω_n is the natural frequency and k is the steady-state gain. These parameters are obtained from the identification experiment (Fig. 6). For identification purposes, the controller $C_K(s)$ is chosen as a simple proportional controller with a very small gain. The primary objective is to maintain the motor's revolution within a narrow range around the reference value.

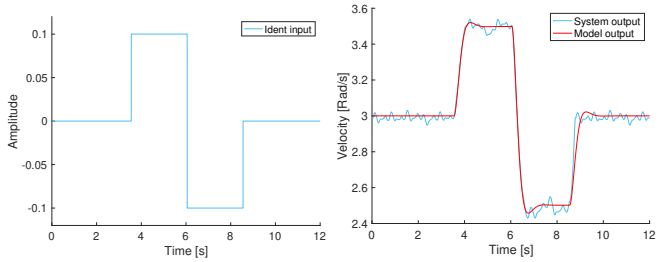

Fig. 6: Identification experiment

The estimated transfer function

$$P(s) = \frac{503}{s^2 + 8.928s + 77.93} \tag{4}$$

will be used as model of the internal current loop for designing control system in the design tool PID H_∞ Designer.

V. Speed Controller Design

The design of the speed controller is divided into several distinct phases. In the first phase, a standard PI controller will be designed. In subsequent phases, this controller will be gradually improved with parallel-connected PR controllers suppressing individual harmonics of periodic disturbances.

Multiple controllers in parallel form - method

To design a controller suppressing periodic disturbances within a given period, we will use the method of gradual controller improvement described in [7]. In this method, we can design analytically a controller with two parameters in each iteration. This approach is applicable to various types of controllers, but in this case, we specifically utilize PI and multiple PR controllers. The fixed structure controller is assumed to be an affine function

$$C(s) \triangleq k_q Q(s) + k_r R(s) + F(s), \tag{5}$$

where $Q(s)$, $R(s)$ and $F(s)$ are arbitrary proper rational transfer functions and k_q, k_r are parameters to be designed. For further detailed design procedure, please refer to [5], [7] or [17].

PID H_∞ Designer:

PID H_∞ Designer [5] is an advanced web design tool (developed in the MATLAB as a standallone application) for analysis and analytical design of a wide class of controllers. For purpose of this article only design of the PI and PR controllers will be used.

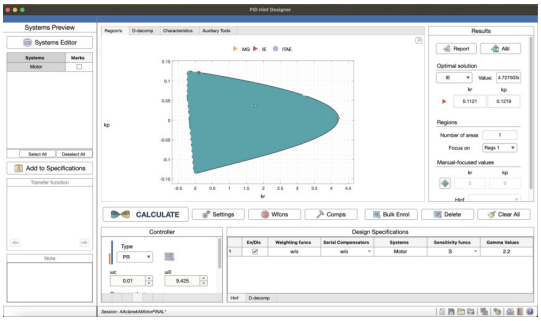

Fig. 7: PID H_∞ Designer

The basic design problem addresses a simple control loop involving a linear, time-invariant, single-input, single-output (LTI-SISO) system. The objective is to determine all controllers of the specific structure with two adjustable parameters, ensuring the internal stability of the loop and fulfilling a predefined H_∞ requirement expressed as an inequality [16]. Each compliant controller is represented as a point in the parametric plane of the controller. The region containing all such points that satisfy the design requirement is referred to as the H_∞ region. The analytical solution to the basic design task entails determining the boundary of this H_∞ region. Subsequently, an additional optimization criterion is employed to select the optimal controller within this region.

In this paper we restrict design requirements on the internal stability of the closed-loop and the limitation of the H_∞ norm of the sensitivity $S(s)$ or complementary sensitivity function $T(s)$ in the form

$$\begin{aligned} |S(j\omega)| &\leq M_S, \quad \forall\omega \in \langle 0, \infty\rangle, \\ |T(j\omega)| &\leq M_T, \quad \forall\omega \in \langle 0, \infty\rangle \end{aligned}$$

or

$$\|S(s)\|_\infty \leq M_S, \tag{6}$$
$$\|T(s)\|_\infty \leq M_T, \tag{7}$$

where $\|H\|_\infty \triangleq \sup_\omega |H(j\omega)|$ is H_∞ norm. This method will be employed for each controller that will be designed in this article.

Iterative process of designing control system:
In this section, we will illustrate a case where we need to suppress three main harmonics of a periodic disturbance. The number of harmonics to suppress can vary; it is up to the designer how and which are chosen. In many cases, it is sufficient to suppress one or two dominant harmonics.

1) PI controller:
The initial step involves designing a standard velocity PI controller that effectively maintains the desired velocity. A proportional-integral controller

$$C_{PI}(s) = k\left(1 + \frac{1}{T_i s}\right) \tag{8}$$

can be obtained as

$$Q(s) = 1, \quad R(s) = \frac{1}{s}, \quad F(s) = 0. \tag{9}$$

In PID H_∞ Designer there are several conditions that can be used to design desired PI controller.

2) PR controller - First harmonic:
After velocity controller deployment, the Fast Fourier Transform (FFT) will be employed to identify the frequency that must be suppressed. For this purpose, it is necessary to determine the frequency of the most significant harmonic component (in our case, it is the first harmonic) of the periodic control deviation corresponding to the PI controller designed in the first step of the design procedure. We suppress this harmonic component in the next step of the design by a PR controller connected in parallel to the already designed PI controller.

Standard form of proportional resonant controller is denoted by

$$C_{PR1}(s) = k_{p1} + k_{r1}\frac{2\omega_{c1}s}{s^2 + 2\omega_{c1}s + \omega_{01}^2}, \tag{10}$$

where ω_{01} is the frequency of the first harmonic to be suppressed, ω_{c1}, $\omega_{c1} << \omega_{01}$, is the design parameter selected by the designer. The smaller ω_{c1} we choose, the greater the gain of the PR controller at the frequency ω_{01}, and the more the disturbance at frequency ω_{01} is suppressed.

$$Q(s) = 1, \quad R(s) = \frac{2\omega_{c1}s}{s^2 + 2\omega_{c1}s + \omega_{01}^2}, \tag{11}$$
$$F(s) = C_{PI}. \tag{12}$$

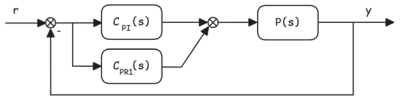

Fig. 8: Closed loop with PI and PR controller

3) PR controller - Second harmonic:
At the beginning of each iteration, the Fast Fourier Transform (FFT) algorithm will be employed. This is because the controller from the preceding iteration will modify the amplitudes of the harmonics. Second PR controller is in form of

$$C_{PR2}(s) = k_{p2} + k_{r2}\frac{2\omega_{c2}s}{s^2 + 2\omega_{c2}s + \omega_{02}^2} \tag{13}$$

where ω_{02} is the frequency of the second harmonic to be suppressed ($\omega_{01} \neq \omega_{02}$). Parameters for following iteration are

$$Q(s) = 1, \quad R(s) = \frac{2\omega_{c2}s}{s^2 + 2\omega_{c2}s + \omega_{02}^2}, \tag{14}$$
$$F(s) = C_{PI} + C_{PR1}. \tag{15}$$

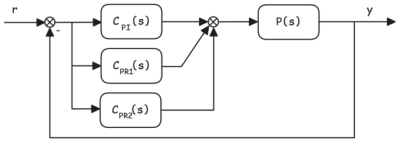

Fig. 9: Closed loop with PI and two PR controllers

4) PR controller - Third harmonic:
Final iteration of this method for case of Education Platform for Periodic Control will be designed for

$$C_{PR3}(s) = k_{p3} + k_{r3}\frac{2\omega_{c3}s}{s^2 + 2\omega_{c3}s + \omega_{03}^2} \tag{16}$$

where ω_{03} is the frequency of the third harmonic to be suppressed ($\omega_{01} \neq \omega_{02} \neq \omega_{03}$). Last setting for final iteration are

$$Q(s) = 1, \quad R(s) = \frac{2\omega_{c3}s}{s^2 + 2\omega_{c3}s + \omega_{03}^2}, \tag{17}$$
$$F(s) = C_{PI} + C_{PR1} + C_{PR2}. \tag{18}$$

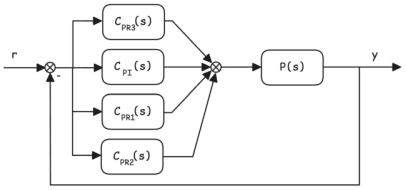

Fig. 10: Closed loop with PI and three PR controllers

Theoretically, iterations can be continued until performance of the control system is satisfactory. Additionally, in certain

instances, it is more convenient to skip harmonics that has a lower or no impact and select next one that have a bigger magnitude. However, for the purposes of this article, we will conclude here.

Speed Controller Design - Example

Iterative process of designing control system will be presented on our motor stand. Initially, transfer function $P(s)$ (4) will be used to design basic PI velocity controller. As mentioned earlier, the PID H_∞ Designer will be used for all of these tasks. Design task is performed by the Table I.

TABLE I: PI velocity controller

Constrains	k_p	k_i
$M_S \leq 1.8,\ M_T \leq 1.2$	0.1491	0.891

The reference value of the motor velocity is set to 3.14 rad/s, which corresponds to one revolution of the motor per two seconds. The Fig. 11 illustrates the velocity error of the motor in rad/s due to presence of magnets.

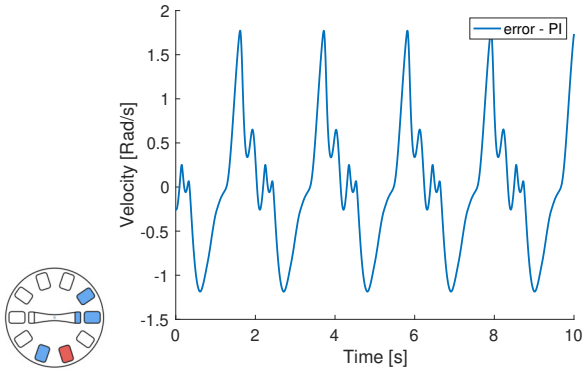

Fig. 11: Periodic disturbance in velocity error

Now the iterative process of designing parallel PR controllers will be utilized. On the Table II, there are all parameters, that are necessary for this process.

TABLE II: PR controller

	Constrains	ω_0	ω_c	k_p	k_r
$PR1$	$M_S \leq 1.95$	3.14	0.01	0.03925	6.212
$PR2$	$M_S \leq 2$	6.28	0.01	0.0.0853	3.84
$PR3$	$M_S \leq 2.1$	9.425	0.01	0.0057	2.027

On figures Fig. 12 and Fig. 13 there are comparisons between each iteration. The most substantial difference is after adding the first PR controller, that suppress main harmonic frequency at 3.14 rad/s. For example max velocity error is lowered 23 times! Next iterations are improving whole response of motor to periodic disturbances, but difference is not as substantial as adding the first PR controller.

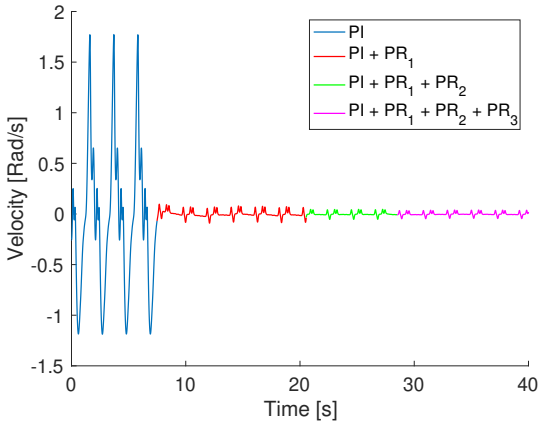

Fig. 12: Periodic disturbance in velocity error

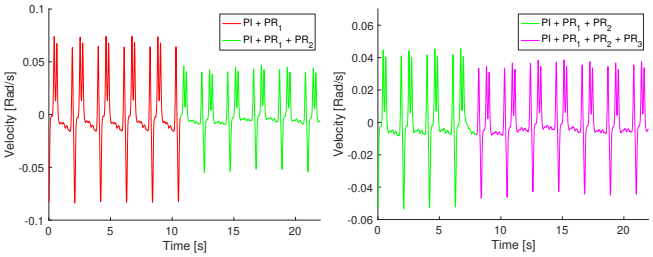

(a) PR1 and PR2 (b) PR2 and PR3

Fig. 13: Periodic disturbance in velocity error

Graphs of selected harmonic spectrum of velocity signal, that are obtained by FFT, are also interesting (Fig. 14 and Fig. 15). Notably, there is a significant improvement here. The first figure depicts the selected harmonic spectrum of the velocity error signal with a PI controller and a PI + PR controller. The Fig. 15 illustrate the precise improvements achieved by selectively enhancing each dominant harmonic.

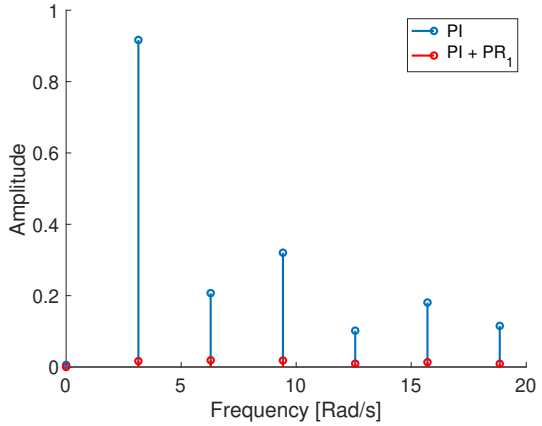

Fig. 14: Selected harmonic spectrum of velocity error signal

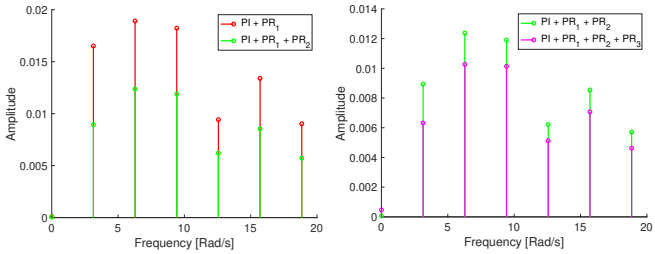

(a) PR1 and PR2 (b) PR2 and PR3

Fig. 15: Selected harmonic spectrum of velocity error signal

The final Fig. 16 presents the amplitude frequency response of the closed loop for each iteration. The antiresonance peaks indicate the precise frequencies that are attenuated by incorporating PR controllers. Furthermore, it is evident that suppressing additional harmonics will be intricate or even infeasible due to the significant resonance peak.

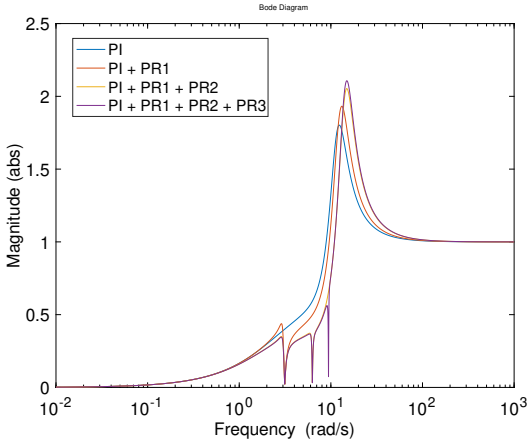

Fig. 16: Amplitude Frequency Response - Comparison

In some other cases, we may continue with iterations, but in this instance, we will conclude the iterations and finalize the controller as a combination of a PI controller and three PR controllers.

From a robustness perspective, generally, PR controllers exhibit significant sensitivity to changes in the frequency of the exogenous signal. However, as evident from Fig. 16, even with a substantial change in frequency, the performance of the final controller surpasses that of a simple PI controller (within the controller's working range).

VI. Conclusion

This paper describes a comprehensive platform for teaching and developing controllers that suppress disturbances within a given period. This platform includes a low-cost physical model - a 3D-printed Periodic Motor Stand Model - and all the necessary software tools needed to develop a speed controller that suppresses periodic disturbances within a given period. The authors believe that the teaching platform presented in the paper is very useful for teaching and developing periodic and repetitive control systems.

Acknowledgements

This work was supported by project DigiTech, grand agreement No.23 021/0008436-01.

References

[1] K. Toyama, H. Ohtake, S. Matsuda, S. Kobayashi, M. Morimoto and H. Sugimoto, "Repetitive control of current for residential photovoltaic generation system, 2000 IEEE International Conference on Industrial Electronics, Control and Instrumentation. 21st Century Technologies, Nagoya, Japan, 2000, pp. 741-745 vol.2.

[2] M. Goubej and M. Schlegel, "PI Plus Repetitive Control Design: H-infinity Regions Approach," 2019 22nd International Conference on Process Control (PC19), Strbske Pleso, Slovakia, 2019, pp. 62-67, doi: 10.1109/PC.2019.8815312.

[3] H. Cha, T. -K. Vu and J. -E. Kim, "Design and control of Proportional-Resonant controller based Photovoltaic power conditioning system," 2009 IEEE Energy Conversion Congress and Exposition, San Jose, CA, USA, 2009, pp. 2198-2205, doi: 10.1109/ECCE.2009.5316374.

[4] REX Controls s.r.o. REXYGEN Control System [Online]. Available: https://www.rexcontrols.com

[5] PID H_∞ Designer [Online]. Available: https://www.pidlab.com

[6] Ljung, L. System Identification: Theory for the User, Appendix 4A, Second Edition, pp. 132–134. Upper Saddle River, NJ: Prentice Hall PTR, 1999.

[7] M. Brabec and M. Schlegel, "Analytical Design of a Wide Class of Controllers with Two Tunable Parameters Based on H-∞ Specifications," 2023 24th International Conference on Process Control (PC), Strbske Pleso, Slovakia, 2023, pp. 221-226, doi: 10.1109/PC58330.2023.10217459.

[8] Y. Shi and J. Su, "An active damping method based on PR control for LCL-filter-based grid-connected inverters," 2014 17th International Conference on Electrical Machines and Systems (ICEMS), Hangzhou, China, 2014, pp. 944-948, doi: 10.1109/ICEMS.2014.7013604.

[9] V. Šetka and D. Tolar, "Motor controller designed for robotics based on microcontroller with integrated EtherCAT," 2018 19th International Carpathian Control Conference (ICCC), Szilvasvarad, Hungary, 2018, pp. 289-294, doi: 10.1109/CarpathianCC.2018.8399643.

[10] W. Jian, W. Zhi-qiang, L. Guo-feng, W. Ning-hui and W. Jin-jun, "PI-Repetitive control applied to three-phase four-wire active power filter," 2017 36th Chinese Control Conference (CCC), Dalian, China, 2017, pp. 10751-10756, doi: 10.23919/ChiCC.2017.8029070.

[11] A. V. J. S. Praneeth, N. A. Azeez, L. Patnaik and S. S. Williamson, "Proportional resonant controllers in on-board battery chargers for electric transportation," 2018 IEEE International Conference on Industrial Electronics for Sustainable Energy Systems (IESES), Hamilton, New Zealand, 2018, pp. 237-242, doi: 10.1109/IESES.2018.8349880.

[12] M. Pallantla and R. S, "Input Power Proportional Control of LLC Resonant Converter," 2024 IEEE Transportation Electrification Conference and Expo (ITEC), Chicago, IL, USA, 2024, pp. 1-6, doi: 10.1109/ITEC60657.2024.10599081.

[13] Vu, Trung-Kien and Seong, Se-Jin. (2010). Comparison of PI and PR Controller Based Current Control Schemes for Single-Phase Grid-Connected PV Inverter. Journal of the Korea Academia-Industrial cooperation Society. 11. 2968-2974. 10.5762/KAIS.2010.11.8.2968.

[14] M. Alathamneh, H. Ghanayem and R. M. Nelms, "A Robust Three-Phase Shunt Active Power Filter with Frequency Adaptive PR Controller and Sensorless Voltage Control," 2023 IEEE Industry Applications Society Annual Meeting (IAS), Nashville, TN, USA, 2023, pp. 1-8, doi: 10.1109/IAS54024.2023.10406769.

[15] EtherCAT Technology Group. "EtherCAT – the Ethernet Fieldbus". [Online]. https://www.ethercat.org/en/technology.html

[16] P. Apkarian, Dominikus Noll. The H∞ Control Problem is Solved. Aerospace Lab, 2017, 13, p. 1-11.

[17] M. Schlegel and M. Brabec, PID H∞ Designer Introduction [Online]. https://www.pidlab.com/wp-content/uploads/2023/07/pid_hinf_designer_introduction.pdf

[18] Srinivasan, Muralidharan and T., Balasubramaniyam and K.S, Prethesh and C., Aswin. (2023). Performance analysis of controllers in BLDC motor. E3S Web of Conferences. 387. 10.1051/e3sconf/202338701001.

[19] Field-Oriented Control - Mathworks [Online]. https://www.mathworks.com/discovery/field-oriented-control.html